Winter 2-2022

Use of Magnetic Iron-coated Halloysite Nanotubes in Cell Growth, Differentiation, and Combating Cancerous Growth

Christopher Daniel Candler

USE OF MAGNETIC IRON-COATED HALLOYSITE NANOTUBES IN CELL GROWTH, DIFFERENTIATION, AND COMBATING CANCEROUS GROWTH

by

Christopher Daniel Candler, BS

A Thesis Presented in Partial Fulfillment
of the Requirements of the Degree
Master of Science

COLLEGE OF ENGINEERING AND SCIENCE
LOUISIANA TECH UNIVERSITY

February 2022

LOUISIANA TECH UNIVERSITY

GRADUATE SCHOOL

January 7, 2022
Date of thesis defense

We hereby recommend that the thesis prepared by

Christopher Daniel Candler, B.S.

entitled **Use of Magnetic Iron-coated Halloysite Nanotubes in Cell Growth, Differenttiation, and Combating Cancerous Growth**

be accepted in partial fulfillment of the requirements for the degree of

Master of Science in Molecular Sciences and Nanotechnology

David K Mills

David K. Mills
Supervisor of Thesis Research

gergana nestorova

Gergana G. Nestorova
Head of Molecular Sciences and Nanotechnology

Thesis Committee Members:
David K. Mills
Teresa A. Murray
Sven Eklund

Approved:

Hisham Hegab
Dean of Engineering & Science

Approved:

Ramu Ramachandran
Dean of the Graduate School

GS Form 13
(01/20)

ABSTRACT

Magnetic Halloysite Nanotubes can be used in multiple ways in combating growth of osteosarcoma. The adsorption ability of the inner and outer surfaces of halloysite nanotubes allows for attachment of different molecules, including anti-cancer drugs, polymer layering for controlled drug release, and magnetic coating. This magnetic coating would allow for cell membrane disruption, hyperthermia, and for targeting of specific tissue. In this project, the goal was to create these magnetic nanotubes and test their cytotoxicity against stem cells and osteosarcoma cells.

To create these magnetic nanotubes, we used electrodeposition to adsorb ferrous oxide nanoparticles (FeNPs) onto halloysite nanotubes (HNTs) to create iron-coated halloysite nanotubes (FeHNTs). These FeHNTs were then imaged using a field emission scanning electron microscope (FESEM) and underwent elemental analysis, using the energy dispersive X-ray spectroscopy (EDS), to ensure placement of the FeNPs onto the HNTs.

The FeHNTs were then tested for their cytotoxicity and cell differentiation potential against human adipose-derived mesenchymal stem cells (hASCs) and mouse osteosarcoma cells. The viability of both cell lines was compared. Next, the proliferation capability, the potential tissue formation, and the potential ossification of hASCs was compared with increasing concentrations of FeHNTs.

APPROVAL FOR SCHOLARLY DISSEMINATION

The author grants to the Prescott Memorial Library of Louisiana Tech University the right to reproduce, by appropriate methods, upon request, any or all portions of this Thesis. It is understood that "proper request" consists of the agreement, on the part of the requesting party, that said reproduction is for his personal use and that subsequent reproduction will not occur without written approval of the author of this Thesis. Further, any portions of the Thesis used in books, papers, and other works must be appropriately referenced to this Thesis.

Finally, the author of this Thesis reserves the right to publish freely, in the literature, at any time, any or all portions of this Thesis.

Author _____

Date _____

DEDICATION

This thesis is dedicated to my family and friends. Your support is priceless, and I can not thank you enough for it.

TABLE OF CONTENTS

LIST OF FIGURES

LIST OF TABLES

ACKNOWLEDGMENTS

These projects were made possible because of the mentorship, dedication and encouragement of my advisor Dr. David K. Mills. I further acknowledge the wisdom provided to me by my lab mates, all of whom have inspired me and taught me valuable lessons in this pursuit. I pray that I can one day return the favor.

CHAPTER 1

INTRODUCTION

1.1 Treating Osteosarcoma

Osteosarcoma, formerly a grim diagnosis, is still a particularly dangerous form of cancer that requires diligent observation and aggressive treatment. Presenting as a form of abnormal growth, commonly seen in the long bones of the patient, it can cause significant pain and swelling of the area, as well as potentially causing fracture of the bone [1]. If left to metastasize, it has a high chance to become present in the lungs, which will reduce the percentage of survival for the patient [1,2].

Originally, the treatment of osteosarcoma involved the complete amputation of the affected limb. Current treatment has advanced, requiring resection of the tissue affected as well as pre- and post-resection chemotherapeutic treatments. The usage of multiple anti-osteosarcoma agents has shown to improve patient outcomes as well. Unfortunately, resection of the affected tissue requires the removal of healthy tissue near the affected area, to ensure that there is no recurrence of the cancer [1,2]. Such methods require the patient to undergo further medical procedures in order to restore healthy tissue to the affected area. Should the cancer be present again in the same area while the patient is recovering, there is little that can be done to eliminate it and further prevent recurrence.

1.2 Magnetic Nanomaterial

I theorize that through a novel magnetic material, there is potential for a magnetic nanomaterial to be developed that would be used to help combat and prevent growth of osteosarcoma cells, as well as help support the growth of cells necessary to allow for healthy tissue growth. In this paper, I will explore how this magnetic nanomaterial was developed and tested for cell viability for normal cells and osteosarcoma cells, as well as the cell proliferation and tissue formation for the normal cells.

CHAPTER 2

BACKGROUND

2.1 Literature Review

2.1.1 Osteosarcoma

Osteosarcoma is an aggressive cancer that has the potential to kill the affected patient within months. It is also tenacious, with recurrence of the disease occurring in 20-30% of patients in which the cancer is localized. Should the disease undergo metastasis, the recurrence rate increases to 80%. With the addition of adjuvant chemotherapy, patient outcomes have increase from an 11% survival rate to a 61% survival rate, depending upon the stage of the cancer [2]. Should the cancer metastasize in the lungs, which occurs in 85% of cases, the survival rate decreases greatly [1]. However, localized hyperthermia has been studied for use in aiding chemotherapeutic treatments. In one study, patients had a notable increase in their two- and four-year survival rate. In fact, 51 patients out of the 343 patients in the studied showed no detectable disease after treatment, compared to 46 patients showing no detectable disease for chemotherapeutic treatment alone [3].

Diagnosis of potential osteosarcoma sites are necessary in developing an effective treatment plan. Use of radiography and CT scans allow for efficient imaging of not only the affected site, but the type of osteosarcoma affecting the patient. Intraosseous osteosarcoma is the most common form, being highly aggressive in destroying the cortical bone. It is common to find malignant masses in adjacent tissues [4].

Even with the increase in survival rate, there is still the necessity for tissue reconstruction after the required resection of affected tissue. Usually, during resection, a significant amount of healthy tissue is taken with the affected tissue to reduce the chance of recurrence. Afterward, tissue reconstruction surgery is performed, and the patient cannot undergo chemotherapy until the wound is healed, which takes a minimum to 2 – 3 weeks [2]. To combat osteosarcoma more efficiently, the usage of a material that allows for healthy cell growth while limiting osteosarcoma growth is necessary.

2.1.2 Magnetism and Iron Nanoparticles

Currently, there are many uses for magnetics and iron nanoparticles (FeNPs), especially in imaging. For instance, dextran coated FeNPs are used in as a contrast agent for MRIs, being biocompatible and can be excreted after imaging [5]. As well, these same nanoparticles can be used for tracking stem cells using MRI or even causing migration of these stem cells [6, 7]. In multiple studies performed by Xia, et al., they were able to show that magnetic fields, in conjunction with FeNPs, were able to enhance the osteogenic activity of stem cells [8-10]

Magnetics can also potentially be used to combat osteosarcoma growth. In Shen et al., 2016, the authors state that there are many studies that show that electromagnetic field (EMF) exposure can induce many different methods of cell death. In particular, the authors wanted to see the effects exposure to a weak magnetic field would have on macro-autophagy, the ability for the cell to “eat” itself. The authors used Chinese hamster lung (CHL) cells divided into three groups: a positive control group that was treated with 4-nitroquinoline 1-oxide (4NQO) and underwent no exposure to EMF, a group exposed to EMF, and a group exposed to offset EMF called the “sham group”. The cell culture

conditions were 37 ºC and 5% CO2 for all groups, including during EMF exposure testing. It was found that presence of LC3 markers was high after EMF exposure for 24 hours, signaling the presence of autophagic activity. As well, exposure to EMF did cause the surface properties of the cells to change. However, exposure to the EMF did not cause double strand breaks in the cell nucleus and could not induce apoptosis in the target cells [11].

In another study, researchers showed that EMF exposure can influence growth and viability of cancer cells. Authors in Ashdown et al., 2020 theorized that pulsed magnetic fields would have a damaging effect to cancer cells while leaving normal cells alone due to influencing the behavior of the glycocalyx. It has been shown that cancer cells produce more glycosaminoglycans (GAGs) and glycoproteins due to an abnormal glycocalyx. Knowing this, authors used the human lung carcinoma cell line A549, human lung lymphatic endothelial cells (hLEC), Lewis lung carcinoma (LLC) cells, and human breast carcinoma cells (MDA-MB-231). Using a solenoid magnet connected to a circuit to create the necessary pulses for the magnetic fields, all four cell lines were exposed to EMF with a gauss meter used to measure EMF strength. Immediately after being exposed to EMF at frequencies of 50 and 385 Hz and field strength of 20 mT, A549 cells presented protease outside of the cell membrane. This would dictate that the cell membrane had ruptured and was leaking. Shown in Figure 2, the EMF pulses lowered the viability and cell growth of A549 cells. MDA-MB-231 and LLC cell lines showed similar releases of protease, indicating the rupture of the cell membrane. However, hLECs, the only non-cancer cell line and the cell line that would be found near lung adenocarcinoma, showed no differences between the control and the EMF exposed samples in terms of cell

proliferation and viability. This would show that regular cells may very well be able to resist the effects that EMF pulses had on cancerous cells [12].

2.1.3 Magnetic Halloysite Nanotubes

The addition of halloysite nanotubes (HNTs) allows for an expansion of uses for magnetism and iron nanoparticles. One of these uses is controlled and sustained drug delivery. In Fizir, et al., 2017, the authors showed a potential delivery system using magnetic nanoparticles and HNTs. The authors first simulated the interactions between four different monomers and the antibiotic drug Norfloxacin (NOR), settling on the two monomers that had the highest interaction energies. Following simulation of the materials to determine the best composition for the drug delivery, the authors were able to use the HNTs' negatively charged outer surface to attach the positively charged iron ions by adding the HNTs in deionized water with dissolved ferric chloride hydrate ($FeCl_3 \bullet 6H_2O$) and ferrous sulfate hydrate ($FeSO_4 \bullet 7H_2O$) to create magnetic HNTs (MHNTs). Authors then dissolved NOR in acetic acid to allow NOR to attach to the outer surface of the MHNTs. They then coated the NOR-MHNTs with ethylene glycol dimethacrylate (EGDMA) and either methacrylic acid (MAA) or acrylamide (AM), to allow for sustained release of NOR. The authors successfully showed that the release of NOR could be controlled by pH difference, that the release of NOR could be sustained by the composition and concentration of polymers attached to the surface of the NOR-MHNTs, and that the MHNTs could be successfully moved and held by way of magnetism [13].

Antibiotics are not the only drug that can be used in targeted and sustained drug release. In Dramou et al., 2018, researchers were able to use MHNTs to deliver Camptothecin (CPT), an antitumor drug that can be used against a variety of cancers.

CPT itself is difficult to administer, necessitating the need for a delivery system. Using a method similar to Fizir, et al., 2017 to develop MHNTs, the authors then added the MHNTs to a chitosan oligosaccharide (COS) solution so that COS could be added to the outer surface of the MHNTs (COS/MHNTs). Next, the authors dissolved 1-ethyl-3-(dimethylaminopropyl) carbodiimide (EDC) and folic acid (FA) in phosphate buffered saline (PBS), then added the MHNTs into the solution (FA-COS/MHNTs). The FA-COS/MHNTs were separated from the PBS and washed with distilled water then freeze-dried. Finally, CPT was added to the FA-COS/MHNTs to created CPT@FA-COS/MHNTs. Through magnetic testing, the authors were able to prove that the FA-COS/MHNTs had a magnetic field similar to that of Fe nanoparticles. At pH 5, the FA-COS/MHNTs were able to almost release CPT completely in a sustained manner over three days. It was also seen that higher concentrations of FA-COS/MHNTs had worse cell viability against human epithelial colorectal adenocarcinoma cells (Caco-2). It is important to note that in this case, worse cell viability would be preferred against Caco-2 cells. Given this information, CPT that wasn't attached to FA-COS/MHNTs had better outcomes than CPT@FA-COS/MHNTs. However, given the difficulty of administering free CPT to a patient, the near similar efficacy of CPT@FA-COS/MHNTs to free CPT, and the sustained release controlled by pH, this study demonstrates that the FA-COS/MHNTs would make for a sufficient delivery system for anticancer treatment [14].

2.1.4 Stem Cells and Regenerative Medicine

Due to the need for surgical resection to take a large amount of healthy tissue, this requires the patient to undergo reconstructive therapies to replace the taken tissue. As stated before, continuation of chemotherapeutic treatments requires that the surgical

wound be healed first. This necessity opens an avenue for the use of regenerative medicine to allow the patient to heal and start chemotherapy quicker.

Regenerative medicine often requires the use of stem cells from the patient to facilitate repair of the damaged tissue. Originally, mesenchymal stem cells (MSCs) derived from patient bone marrow were used for this endeavor. In fact, bone-marrow-derived MSCs are still used as standard for which stem cells can be used to replace the multiple tissues of the body. MSCs can differentiate into many different cell types, able to undergo osteogenesis, adipogenesis, and chondrogenesis, among others, given environmental conditions [15, 16].

Given the proximity of the extraction area for bone-marrow-derived MSCs and the difficulty and pain associated with retrieval, there would be a need to choose a new tissue to derived MSCs from. Adipose-derived MSCs (hASCs) supply a way to easily and safely extract MSCs through lipoaspiration. In addition to the ease of extraction, hASCs are very proliferative and able to differentiate into the same cell lines as bone-marrow-derived MSCs, making them incredibly useful for regenerative medicine, as well as tissue reconstruction after surgical resection [17 – 19].

Currently, there are many examples for the use of MSCs in the regeneration of lost tissue. For instance, Mills et al. [20] describes the use of composite hydrogels to influence the differentiation and placement of hASCs. Hydrogels encompass a variety of materials that can be used in biomedical applications, with the ability to be developed with a broad range of mechanical and chemical properties. Such materials create microenvironments that can significantly influence cell behavior, as well as acting as a scaffold for tissue regeneration. To even further influence cell behavior, other materials

can be added to the hydrogel. This could not only allow for quick proliferation and differentiation of the hASCs but can also allow for limiting microbial infection or even allowing for sustained drug delivery to the area [20].

CHAPTER 3

IRON-COATED HALLOYSITE NANOTUBES

3.1 Introduction

Iron-coated Halloysite Nanotubes (FeHNTs) provide a unique and cost-effective material for the potential to combat cancerous growth.

3.2 Materials and Methods

3.2.1 Ferrous Oxide Nanoparticles

Ferrous Oxide (Fe3O4), also known as magnetite, has interested scientists throughout the ages due to its significant magnetic properties. Containing equal amounts of iron (II) oxide (FeO) and iron (III) oxide (Fe_2O_3), Fe_3O_4 presents the unique property of ferrimagnetism [21]. Ferrimagnetism is present when the electronic spins are antiparallel (directions are parallel but going in opposite directions), but the magnitude of the spins are different and do not cancel each other [22]. This is due to the two different iron oxides' positioning in Fe_3O_4 crystal structure. This allows for ferrimagnetism to present like ferromagnetism, the classic and most known form of magnetism. Ferrimagnetic materials are naturally attracted to magnets and have the potential to become permanent magnets themselves.

3.2.2 Halloysite Nanotubes

Halloysite nanotubes (HNTs) have been gaining more usage in biomedicine due to their inherently low toxicity, significant biocompatibility, and their able to adsorb different materials due to the different charges of their outer surface and inner lumen. With a length in the range of 0.5 – 1.5 μm, an inner lumen between 10 – 20 nm, and an outer diameter of 40 – 70 nm, HNTs provide a structure that is large enough to hold a significant amount of material and small enough to be used without detriment to cells and tissues [23].

HNTs are rolled sheets of aluminosilicate sheets, with the inner lumen containing aluminol groups and the outer surface containing silicate groups. This unique structure causes the inner and outer surfaces to have different charges, with the inner surface having a positive charge and a pH of around 8.5, and the outer surface having a negative charge and a pH of around 1.5 [24]. These surfaces charges can also be enhanced or reduced to the pH of the environment the HNTs are in. This is useful in the adsorption of different materials to the surfaces of the HNTs, with the materials being adsorbed positioning itself on the surface of with the corresponding charge.

HNTs are also non-cytotoxic, making them perfect carriers for a multitude of drugs, especially cancer drugs. This has been shown in many cases such as in Karewicz et. al. [25], where researchers were able to adsorb Artemisinin, Methotrexate, and Taurolidine, all of which are anti-osteosarcoma drugs, onto the surface of HNTs [25]. In Dramou et. al. [14], where researchers were able to adsorb Camptothecin, an anti-colon cancer drug, to the surface for magnetic HNTs. In addition to loading Camptothecin on the surface of the HNTs, researchers were able to layer different polymers to the surface

for sustained delivery of the drug to the affected area [14]. Finally, HNTs are significantly inexpensive, costing between $600 and $3000 depending upon the application [26].

3.2.3 Development of Iron-Coated Halloysite Nanotubes

Electrodeposition is a relatively simple method of attached nanoparticles to the surface of an HNT. A one-liter beaker was filled with 700 mL of distilled water at a temperature between 80 – 90 °C. Electrodes attached to a 120 V power supply and a stainless-steel stirrer were then added to the beaker, and the water was stirred at around 120 rpm. The stainless-steel stirrer was used instead of a magnetic stirrer to avoid the FeNPs becoming magnetized to the bottom of the beaker or the stirrer. HNTs and FeNPs were then ground together using a pestle and mortar. This is shown in **Figure 3-1**. When sufficiently ground and mixed, the FeNPs and HNTs were then poured into the water and the power supply turned on.

Every five minutes, the power supply would be shut off and the electrodes switched to allow a change in the electrical field of the beaker. This process was done six times in the process. After the end of the final five minutes, the power supply and the stirrer were shut off. The beaker was allowed to cool for five minutes, allowing the material to settle to the bottom of the beaker. Afterward, the supernatant was removed, and the material washed three times with distilled water, then dried at 50°C.

3.2.4 Iron-Coated Halloysite Nanotube Characterization

The resulting material was then imaged using the Hitachi S-4800 FESEM. First, the material was set on carbon tape then blown with puffs of air to dislodge loose

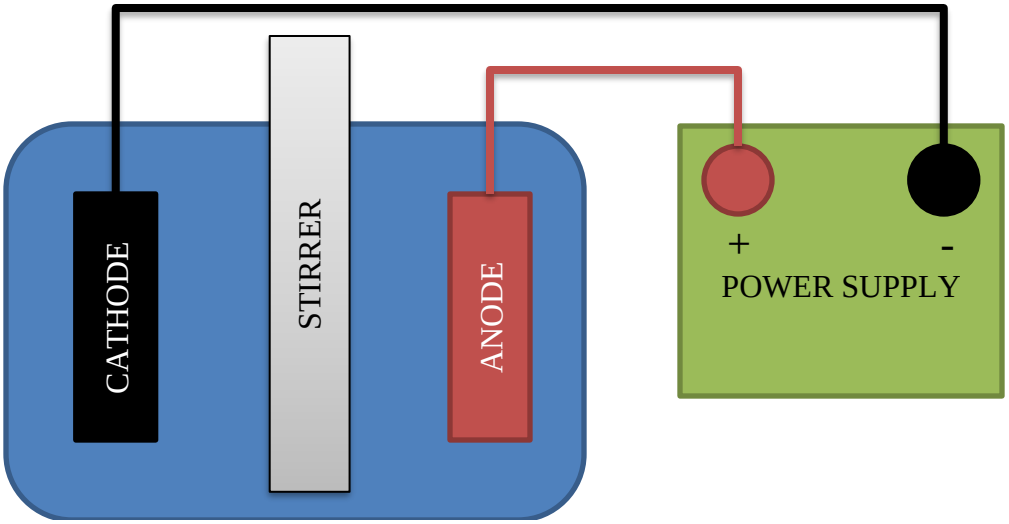

Figure 3-1: Illustration of electrodeposition setup.

material. Afterward, a small magnet was hovered above the material to remove any loose material from the carbon tape. Once it was shown that the material was sufficiently attached to the carbon tape, the material was then layered with 5 nm of gold. This gold layer was used to reduce charging, and subsequent heating, of the potential material. Finally, the material was then placed in the SEM and imaged with an emission current of 9 μA, an accelerating voltage of 3 kV, and a working distance of 8.3 mm. Measurements of the material was taken using ImageJ.

After imaging, the sample then underwent elemental analysis using the Hitachi S-4800 FESEM's Energy Dispersive X-ray Spectroscopy (EDS) system. The analysis used the same conditions as the SEM imaging, except the accelerating voltage was set to 15 kV. Elemental analyses were taken for both the imaged area, as well as specific points in the area.

3.2.5 Iron-Coated Halloysite Nanotube Magnetic Testing

After characterization of the material was performed with SEM-EDS analyses, the material, as well as FeNPs and a Nickel standard, were then tested for magnetization using a Vibrating Sample Magnetometer. This test would show the magnetization of the sample when introduced to a magnetic field with a strength in the range of -10 to 10 kGauss. This would result in the hysteresis curve for each material for comparison.

3.3 Results and Discussion

3.3.1 Characterization

Through SEM analysis, the deposition of FeNPs on the outer surface of HNTs was shown as probable, due to the morphology of the HNTs themselves. Apart from the abnormal amount of aggregation of the HNTs, the HNTs also had irregular shapes on the outer surface, showing potential FeNP coating, shown in **Figure 3-2**. The potential FeHNTs showed an average length of 852.5 nm and a standard deviation of 228.1 nm, and an average width of 79.6 nm and a standard deviation of 13. 7 nm.

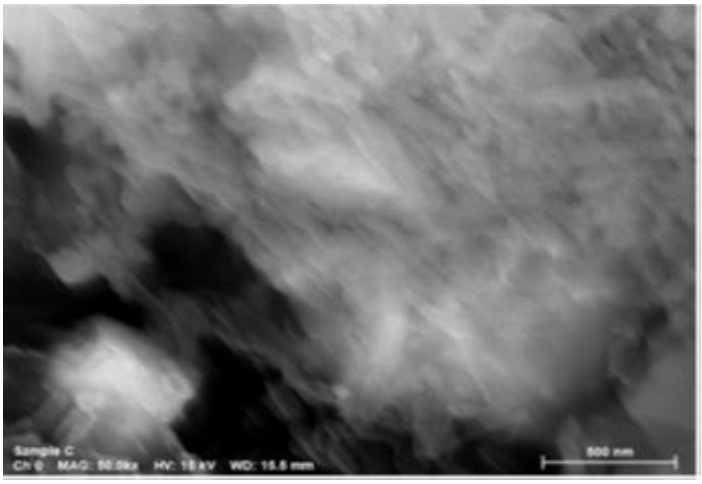

Figure 3-2: Scanning electron microscope image of iron-coated halloysite nanotubes.

EDS analysis confirmed the presence of FeNPs on the surface of the HNTs. Confirmation was shown by elemental maps showing the locations of the FeNPs on the surfaces of the HNTs, as well as through the intensity of the x-ray dispersion from the targeted area, shown in **Figure 3-3**.

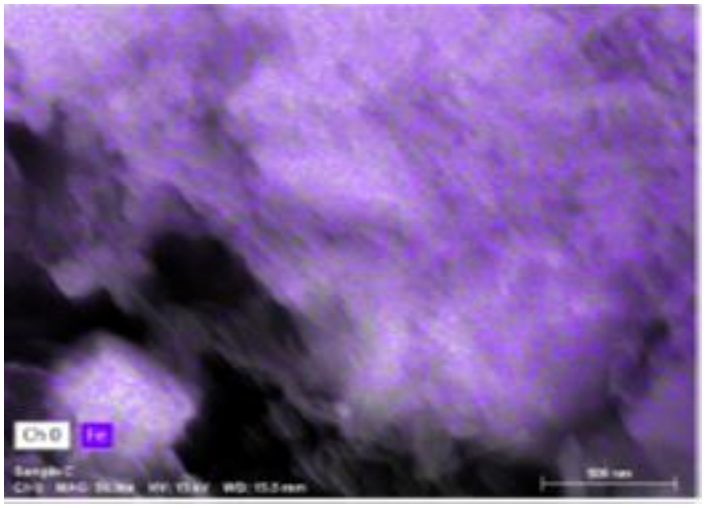

Figure 3-3: Energy dispersive X-ray spectroscopy map of iron-coated halloysite nanotubes.

3.3.2 Magnetic Testing

Magnetic testing through the Vibrating Sample Magnetometer showed a magnetization of 64.177 emu/g in a magnetic field of 10 kGauss, a magnetization of -64.657 emu/g in a magnetic field of -10 kGauss, and an average magnetization of 0 emu/g in a magnetic field of 0 kGauss. This, in fact, proved to have greater magnetization then the nickel standard, but less magnetization then the FeNP control, possibly due to the presence of HNTs. The hysteresis curve showed that the material is, in fact, a ferrimagnetic material, as seen in **Figure 3-4**.

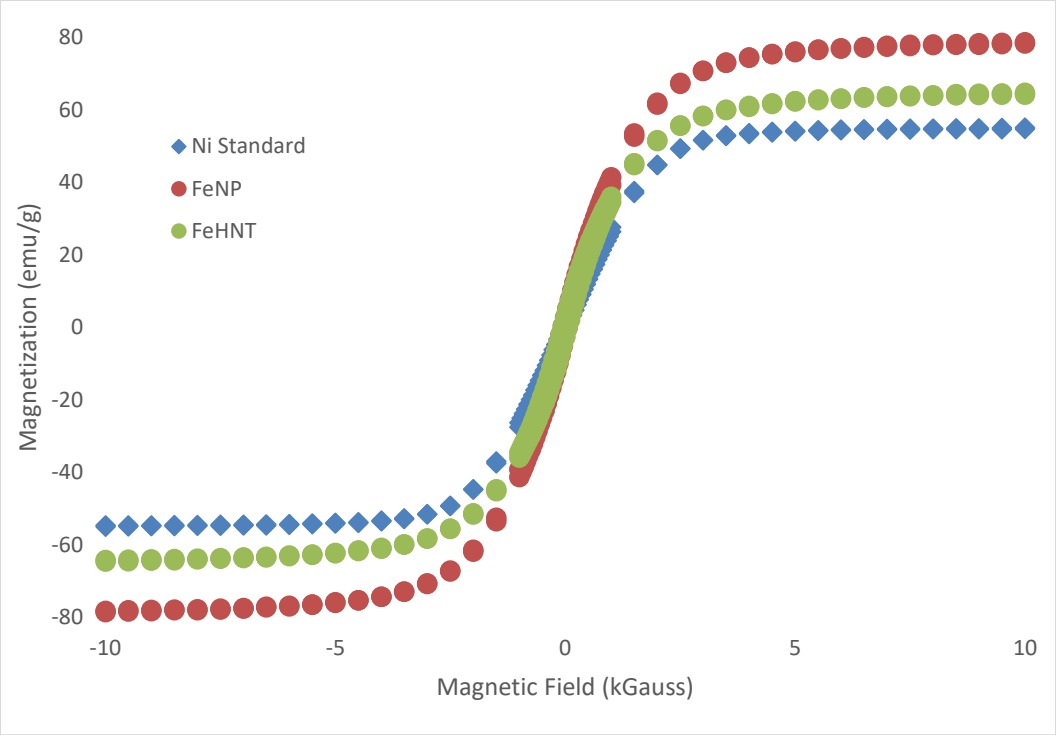

Figure 3-4: The magnetization curves of an iron-coated halloysite nanotube sample and an iron nanoparticle sample compared to a nickel standard.

CHAPTER 4

CELL CULTURE STUDIES

4.1 Introduction

While Fe-HNTs are potentially useful in multiple biomedical applications, it must be confirmed if the material is cytotoxic against osteosarcoma and healthy cells, and if it provides a bias towards differentiation of stem cells into certain cell types. To do this, the cells must be cultured and studied for viability, proliferation, and differentiation.

4.2 Materials and Methods

4.2.1 Cell Lines

The two cell lines used for culturing were human adipose-derived mesenchymal stem cells (hASCs) and mouse osteosarcoma (CRL-2836). hASCs were chosen for their ability to be able to undergo osteogenesis, adipogenesis, myogenesis or chondrogenesis [27]. Both cell lines were also chosen due to their relatively availability and ease of culturing.

4.2.2 Cell Culture Media

The culture media is a mixture of 89% v/v Dulbecco's Modified Eagle Medium (DMEM), 10% v/v Fetal Bovine Serum (FBS), and 1% v/v Penicillin and Streptomycin, totaling to a volume of 500 mL per batch. DMEM is a medium that is often used for cell

lines of those types, while FBS is commonly used to grow different cell lines. Penicillin and Streptomycin are commonly used to protect cells from bacterial infection.

4.2.3 Cell Culturing

Each cell line was defrosted and suspended in 15 mL of culture media before being seeded, at a density of 5e5 cells per mL, in a T75 flask. The cells were placed in an incubator at a temperature of 37 °C, humidity at 95%, and CO_2 at 5%. Every two days the media was drained from the flask and replaced with 15 mL of fresh culture media. When the cells reach 80% confluence, they were passaged using 5 mL of Phosphate-Buffered Serum (PBS) to wash the cells, then 0.5% Trypsin to detach the cells from the surface of the flask. They were then passaged into 2-4 different T75 flasks. Cells were used for cell seeding in all assays after Passage 3. Cells leftover from seeding were frozen and stored in -80 °C freezer. The serial dilution to create all concentrations of the FeHNTs in media is shown in **Table 4-1**.

4.2.4 Cell Proliferation Assay

Cell proliferation assays were performed on hASCs to measure increases in cell populations within two weeks. The cells were placed into 48-well culture plates at a cell density of 1e6 cells per mL of culture medium (5,000 cells per well). The samples were separated by material and concentration. FeHNTs were compared against FeNPs and HNTs, all at concentrations of 5, 10, and 20 µg/mL. As a negative control, cells were placed in culture wells with pure culture media. Each sample was repeated three times, holding 200 µL of media. Every two days, the culture media was drained then replaced with 200 µL of fresh media.

Table 4-1: Serial dilution of iron-coated halloysite nanotubes to make 20 mL of each concentration.

Label	Concentration	FeHNTs (mg)	FH2K (mL)	FH100 (mL)	Media (mL)
FH2K	2 mg/mL	40	-	-	20
FH100	0.1 mg/ml	-	1	-	19
FH50	0.05 mg/mL	-	-	10	10
FH20	0.02 mg/mL	-	-	4	16
FH10	0.01 mg/mL	-	-	2	18

Assays were performed using the CyQUANT™ Cell Proliferation Assay (C7026) on 1, 7, and 14-days after cells were inserted into wells. To create the reagent for the cell proliferation assay, 1 mL of the cell-lysis buffer and 50 µL of CyQUANT™ GR dye was put into 19 mL of distilled water, then vortex. The dye, buffer, and the reagent were protected from light.

When the cells were ready to assay, the plate was drained of media then blotted on paper towels, then frozen in –80 °C for 24 hours to cause cell lysis. The cells were then thawed to room temperature, and then the 200 µL of the reagent was added to each well and incubated at room temperature for five minutes, protected from light. The cells were then put into the fluorescence microplate reader and then evaluated at 490 nm and 540 nm for excitation and emission maxima, respectively.

4.2.5 Viability Assays

In addition to the cell proliferation assays, viability assays were performed on both hASCs and mouse osteosarcoma cell lines. These were performed with 48-well plates and a seeding density of 1e6 cells per mL of culture medium (5,000 cells per well) for hASCs and a seeding density of 5e5 cells per mL of culture medium (2,500 cells per well) for the mouse osteosarcoma cell line. These assays also had the samples separated

by material and concentration, with FeHNTs, FeNPs, and HNTs at concentrations of 5, 10, and 20 µg/mL going against cells seeded in pure media. Each well held 200 µL of media, and all samples were repeated three times. Every two days, the media was drained and then replaced with 200 µL of fresh media.

Assays were performed using the Biotium Viability/Cytotoxicity Assay Kit for Animal Live & Dead Cells (30002-T) at 1, 3, 5, and 7 days after cell seeding. This assay was chosen for is stains: Calcien AM that only stains living cells and Ethidium Homodimer III (EthD-III) that only stains dead cells. Calcien, when viewed using fluorescence microscopy, glows green when attached to cells. EthD-III, on the other hand, stains the cells red. To create the staining solutions, 5 µL of Calcien AM and 20 µL of EthD-III was placed into 10 mL of PBS then vortexed, protected from light.

When ready, the assays were drained of culture media, then washed twice with PBS before adding 200 µL of staining solution to each well. It was then covered with tin foil, then incubated at room temperature for 45 minutes before being imaged using a fluorescence microscope, the FITC filter for viewing the live cells, and the TexasRed filter for viewing dead cells. Cell counts for each were done using ImageJ.

4.2.6 Picrosirius Red Assay

In an effort to understand if hASCs were differentiating and what tissue they were differentiating into, Picrosirius Red assays were performed. These assays were performed in 24-well assays. Instead of comparing different materials are different concentrations to FeHNT, these assays focused on FeHNT at four different concentrations: 10, 20, 50, and 100 µg/mL, all of which were compared against cells in pure culture media. Each sample was repeated three times. Cells were seeded in each well at 5e5 cells per mL of culture

media (2,500 cells per well). Each well held 500 µL of media, and the media was replaced with fresh media every two days.

The assays were dyed with the Picrosirius Red stain from ScyTek Laboratories at 1, 7, and 14 days. Picrosirius Red Stain is used to evaluate potential connective tissues, with the stain being red when staining collagen fibers, and becoming yellow when staining muscle fibers or cytoplasm. Before the stain can be used, however, the cells must be fixed using 2-4% paraformaldehyde for 10-20 minutes.

After fixing, cells were rehydrated using 500 µL of distilled water for 30 seconds. The distilled water is removed, then 500 µL of the Picrosirius Red stain was added to each well, then incubated at room temperature for 60 minutes. The wells were then rinsed twice with 0.5% acetic acid and rinsed once with absolute alcohol. The samples were then dehydrated with absolute alcohol, in well for 15 seconds, before imaging with a phase contrast microscope. After imaging, the stain was then removed from the cells using 10% acetic acid, then its absorbance was measured using an absorbance microplate reader at a wavelength of 490 nm.

4.2.7 Alizarin Red S Assay

In addition to Picrosirius Red assays, Alizarin Red S assays were performed to evaluate potential tissue development. These assays were performed in 24-well assays. Instead of comparing different materials are different concentrations to FeHNT, these assays focused on FeHNT at four different concentrations: 10, 20, 50, and 100 µg/mL, all of which were compared against cells in pure culture media. Each sample was repeated three times. Cells were seeded in each well at 5e5 cells per mL of culture media (2,500

cells per well). Each well held 500 µL of media, and the media was replaced with fresh media every two days.

The assays were dyed with the Alizarin Red S stain from VitroView Biotech at 1, 7, and 14 days. Alizarin Red S stain is used to evaluate potential osteogenic activity, with the stain becoming red when in the presence of calcium. Before the stain can be used, however, the cells must be fixed using 2-4% paraformaldehyde for 10-20 minutes.

After fixing, cells were rehydrated using 500 µL of 70% alcohol for 30 seconds, then rinsed in distilled water. The distilled water is removed, then 500 µL of the Alizarin Red S stain was added to each well, then incubated at room temperature for 5 minutes. The wells were then rinsed twice with 0.5% acetic acid and rinsed once with absolute alcohol. The samples were then dehydrated with absolute alcohol, in well for 15 seconds, before imaging with a phase contrast microscope. After imaging, the stain was then removed from the cells using 10% acetic acid, then its absorbance was measured using an absorbance microplate reader at a wavelength of 405 nm.

4.3 Results and Discussion

4.3.1 Cell Proliferation Assay

Initially, the hASCs had higher cell populations when treated with HNTs, FeNPs, and FeHNTs, with the cell populations increasing greatly from the Day 1 to the Day 7 assays. However, when assayed at Day 14, the increase in cell proliferation had sharply declined, with most of the materials and concentrations having lower cell populations than the control assays. However, the sample containing 5 µg/mL FeNPs had a higher cell population than the control. This is shown in **Figure 4-1**.

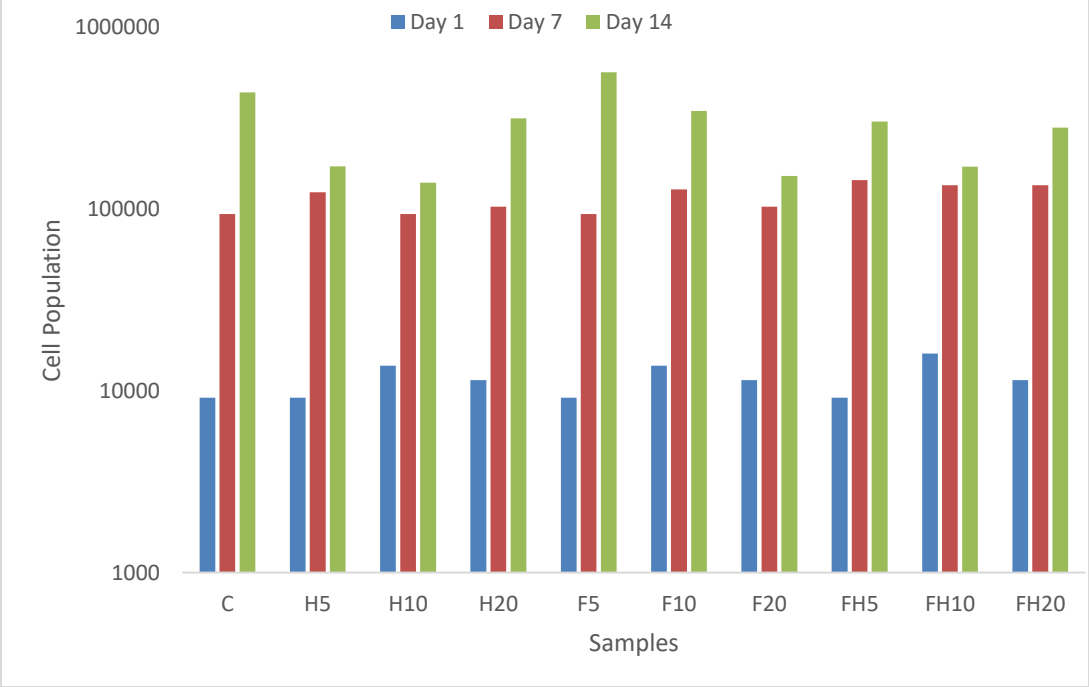

Figure 4-1: Comparison of cell proliferation when samples are exposed to different materials (iron nanoparticles, halloysite nanotubes, and iron-coated halloysite nanotubes) and concentrations of those materials over 14 days.

4.3.2 Viability Assays

Throughout the week, the viability of the hASCs that were treated with FeHNTs were close to the viability of the control samples. There was much more variation for cells treated with FeNPs and HNTs. HNTs showed lower viability than the control sample. However, for all samples, treated or control, the viability started to drop around Day 5. This is shown in **Figure 4-2**, **Figure 4-3**, and **Figure 4-4**. Given that all cells, treated or control, showed a drop in viability, a drop in proliferation after Day 7, and that both assays were done at cells seeded at 5,000 cells per well, it can be concluded that the materials were not the cause of the drops in viability and proliferation, but such drops were caused by over-confluence of hASCs.

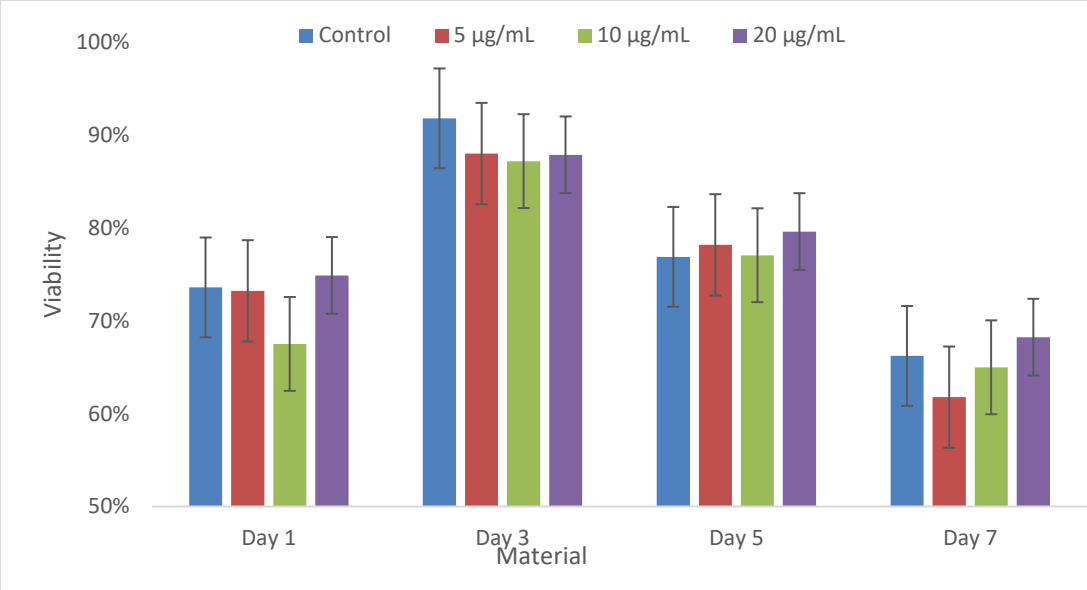

Figure 4-2: Comparison of the viability of human adipose-derived mesenchymal stem cells treated with different concentrations of iron-coated halloysite nanotubes over seven days.

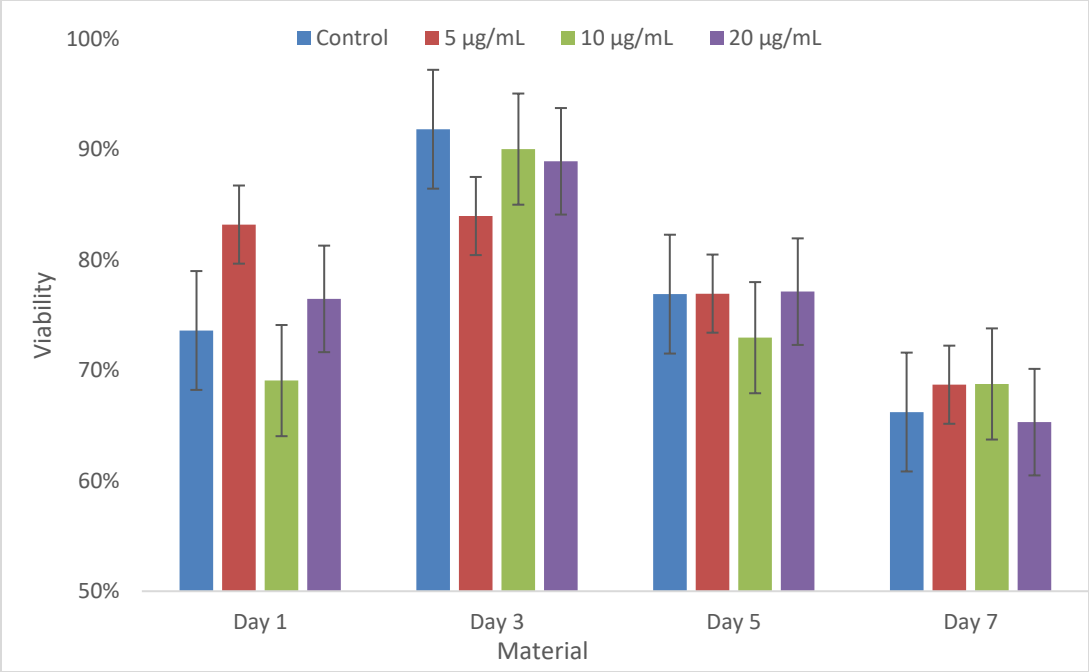

Figure 4-3: Comparison of the viability of human adipose-derived mesenchymal stem cells treated with different concentrations of iron nanoparticles over seven days.

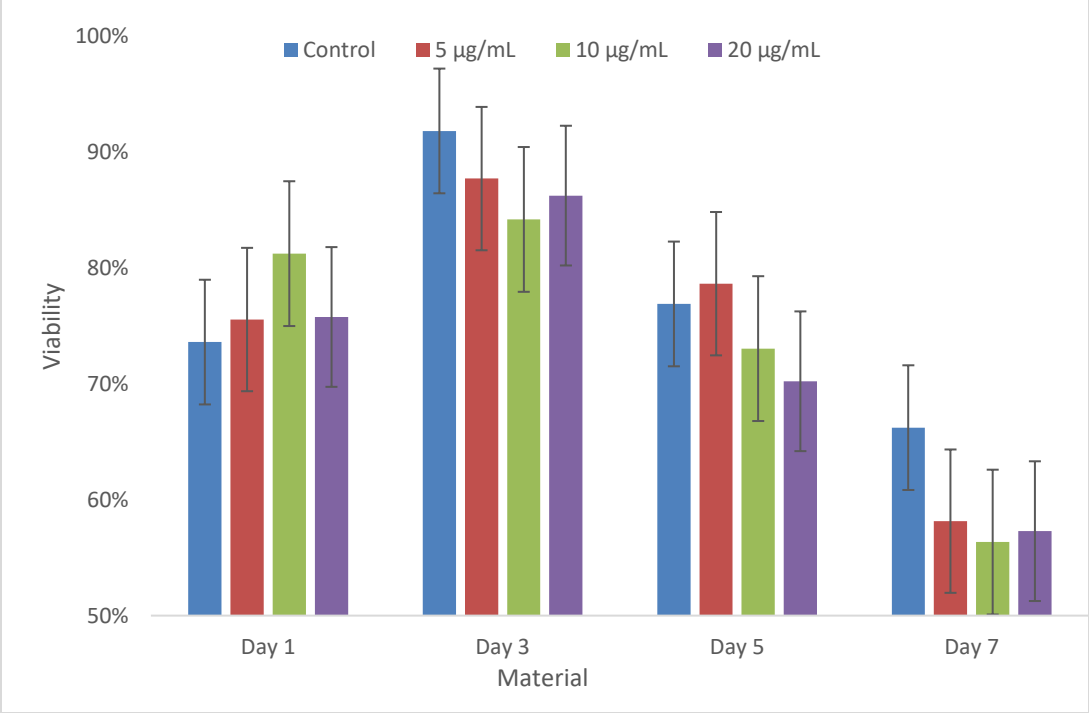

Figure 4-4: Comparison of the viability of human adipose-derived mesenchymal stem cells treated with different concentrations of halloysite nanotubes over seven days.

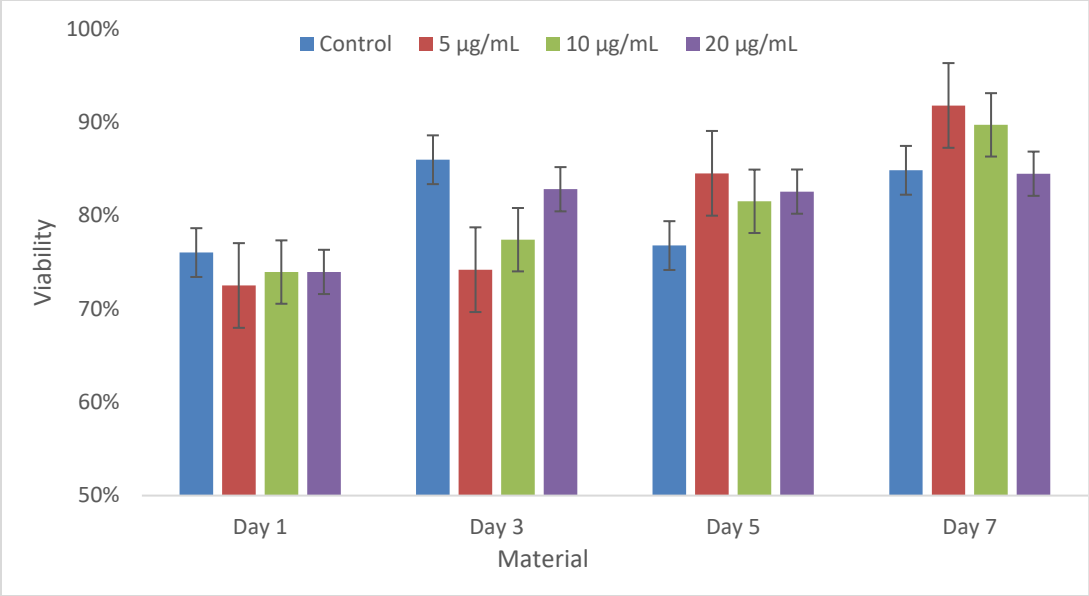

Figure 4-5: Comparison of Osteosarcoma viability subjected to different concentrations of iron-coated halloysite nanotubes over seven days.

This is somewhat confirmed with the mouse osteosarcoma cells as they had lower cell seeding density (2,500 cells per well) and did not show a drop in viability for any of the materials or concentrations, except for the control cells. Osteosarcoma showed a much higher viability after Day 5 when treated with FeHNTs. This is also seen with FeNPS, possibly showing a correlation between iron and an increase in osteosarcoma viability. This is shown in **Figure 4-5**, **Figure 4-6**, and **Figure 4-7**.

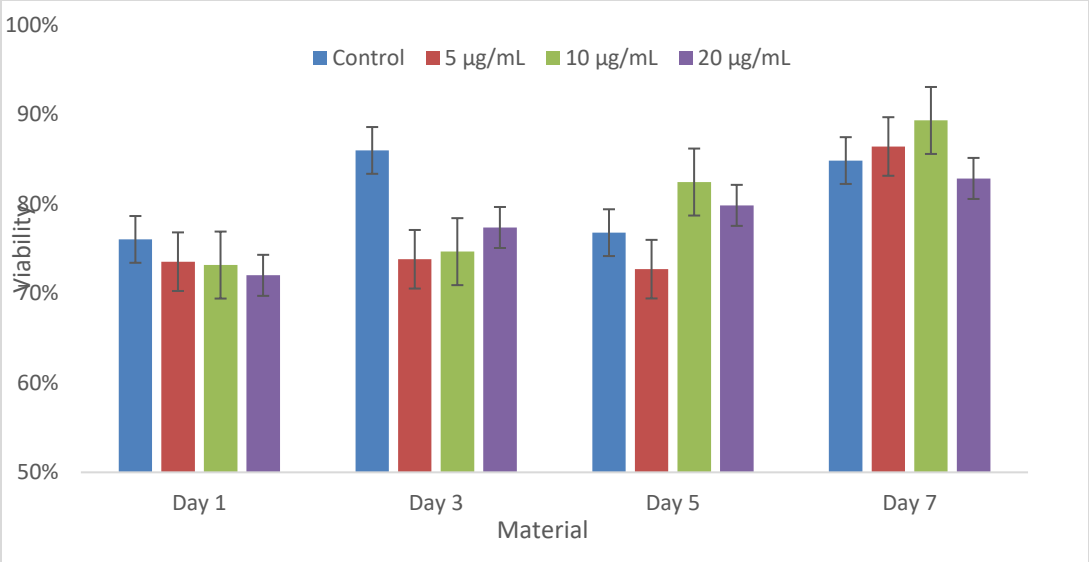

Figure 4-6: Comparison of Osteosarcoma viability subjected to different concentrations of iron nanoparticles over seven days.

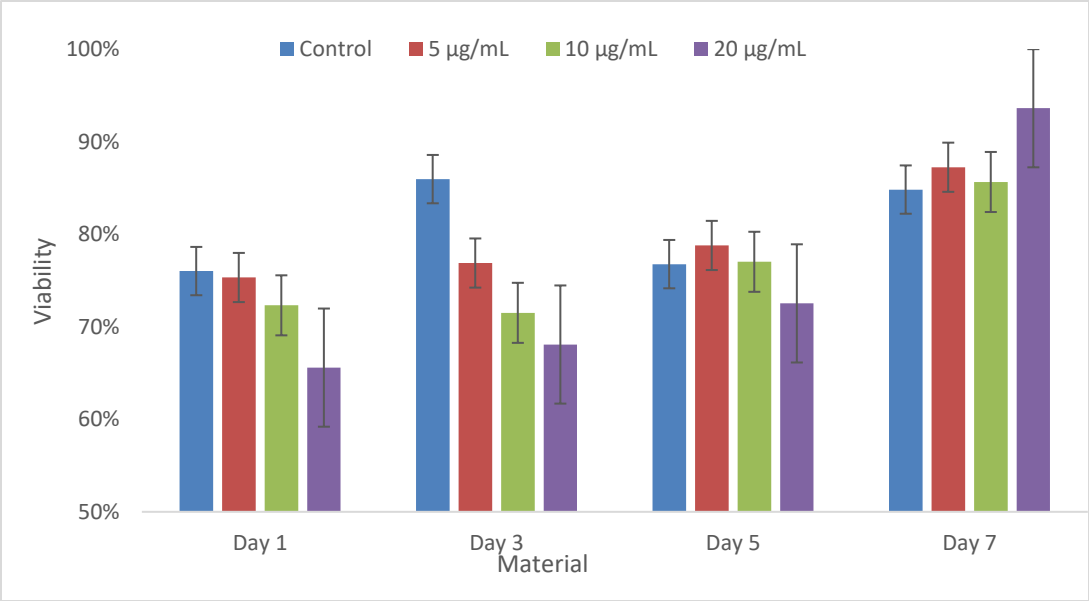

Figure 4-7: Comparison of Osteosarcoma viability subjected to different concentration of halloysite nanotubes over seven days.

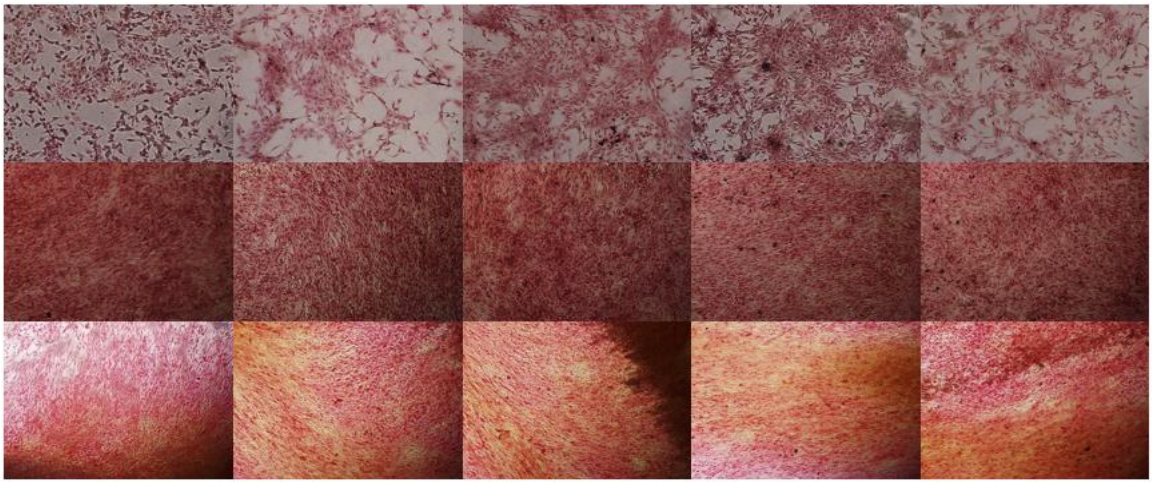

Figure 4-8: Phase contrast images of Picrosirius Red Stain for control cells (left column), cells treated with 10 µg/mL (mid-left column), 20 µg/mL (middle column), 50 µg/mL (mid-right column), and 100 µg/mL (right column) iron-coated halloysite nanotubes on Day 1 (top rom), Day 7 (middle row), and Day 14 (bottom row).

4.3.3 Picrosirius Red Assay

From Day 1 to Day 7, FeHNTs with higher concentrations had higher absorbance, showing an increase in cells for those samples. Viewing the imaging for all samples

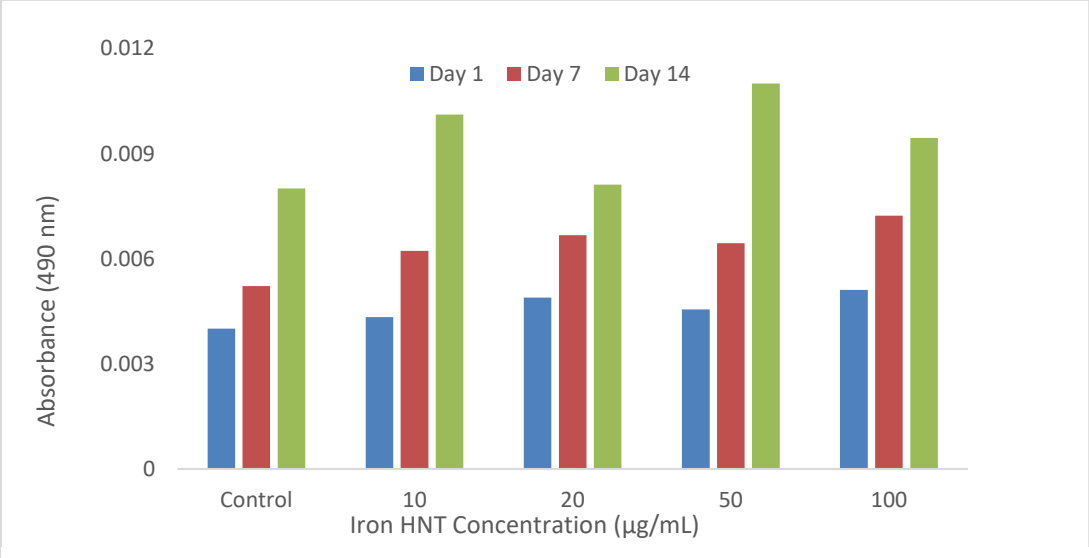

Figure 4-9: Comparison of Picrosirius Red absorbance when human adipose-derived mesenchymal stem cells are exposed to concentrations of 10, 20, 50, and 100 µg/mL of iron-coated halloysite nanotubes over 14 days.

shows initial beginnings of tissue formation for Day 1, potential collagen development at Day 7, and potential collagen maturation at Day 14. This is shown in **Figure 4-8**, and absorbance is shown in **Figure 4-9**.

4.3.4 Alizarin Red S Assay

Throughout the two weeks, negligible amounts of osteogenic activity were viewed, with a negligible amount of calcium viewed in the Day 14 assays. With the low osteogenic activity, increasing only slightly within Day 14, and the potential collagen development and maturation on Day 7 and Day 14, it is possible that the hASCs were undergoing chondrogenesis. Images of the Alizarin Red S assays showed like assays viewed in Tzortzaki et al., 2006 and Gleeson et al., 2010 [28,29]. This is shown in **Figure 4-10**, and absorbance is shown in **Figure 4-11**.

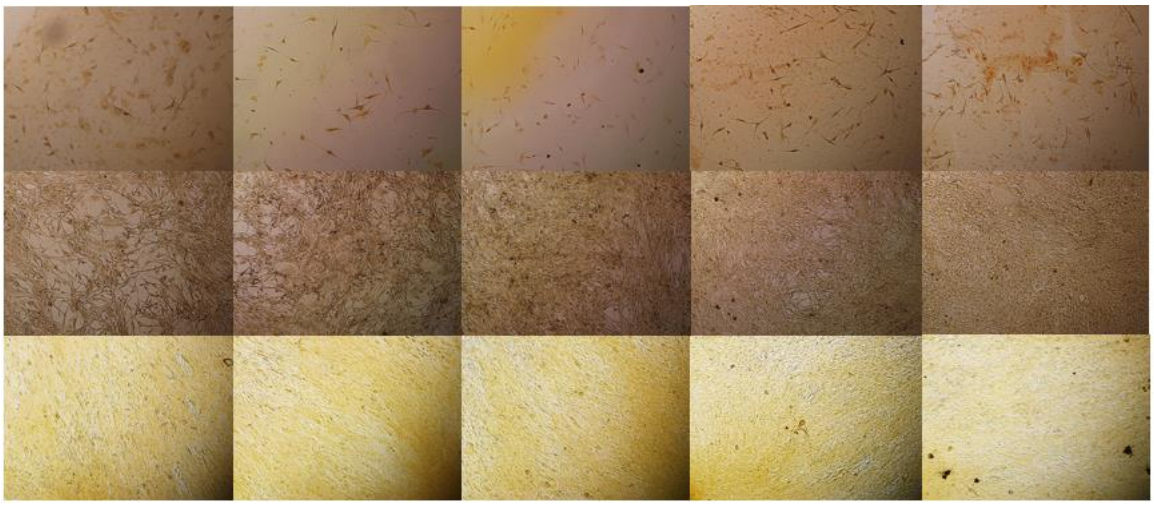

Figure 4-10: Phase contrast images of Alizarin Red S Stain for control cells (left column), cells treated with 10 µg/mL (mid-left column), 20 µg/mL (middle column), 50 µg/mL (mid-right column), and 100 µg/mL (right column) iron-coated halloysite nanotubes on Day 1.

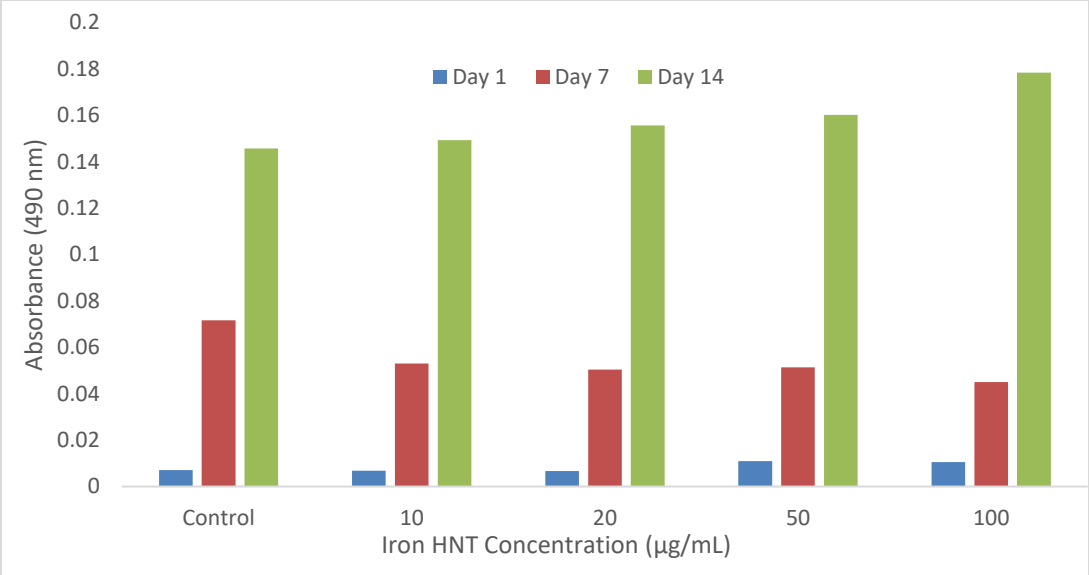

Figure 4-11: Comparison of Alizarin Red S absorbance when human adipose-derived mesenchymal stem cells are exposed to concentrations of 10, 20, 50, and 100 µg/mL of iron-coated halloysite nanotubes over 14 days

CHAPTER 5

DISCUSSION

5.1 Development of Iron-Coated Halloysite Nanotubes

The use of magnetics has been shown to potential to allow for more effective methods to combat osteosarcoma. As such, the development of magnetic nanoparticles could further increase this efficacy and increase patient survivability as well. The development of FeHNTs allows for magnetic nanomaterials that can also be used for controlled drug delivery. This could prove invaluable to not only combating osteosarcoma, but in reducing potential infections and increasing tissue regeneration after surgery. With reduced time of recovery, post-surgical chemotherapy can begin, further eliminating osteosarcoma cells.

The electrodeposition method allows for quick and easy attachment FeNPs to HNTs. The method requires equipment that is not expensive to acquire, with materials that are simple to use and non-cytotoxic. The procedures are easy to perform with little danger to who is developing. Purification of the materials is also very simple, while also allowing for further purification procedures to be added later, should said procedures be needed for more specialized applications. The resulting FeHNTs show the wanted properties from both the HNTs and FeNPs. The iron-coating of the FeHNTs allow for the material to present the ferrimagnetic properties of the FeNPs, while also allowing for the adsorption properties of HNTs. This would allow for sustained and controlled drug

delivery, allowing for anti-cancer drugs to be used before and during wound healing, further increase efficacy.

5.2 Cytotoxicity and Differentiation Potential of FeHNTs

For both hASCs and mouse osteosarcoma cells, FeHNTs showed little to no cytotoxicity, allowing for cell populations and viability to increase, sometimes further than the control cells that weren't treated with FeHNTs. While not limiting the viability and proliferation of osteosarcoma cells is not favored, the material properties of the FeHNTs will allow for greater efficacy in combating cancer cells while not inadvertently damaging the healthy cells. Given the ability for hASCs to proliferate quickly and to be easily and safely be retrieved, as well as its potential to be differentiated into tissues that comprise most of the body, this allows for easier tissue regeneration.

FeHNTs also shows little bias for differentiation, with potential chondrogenesis being shown in experiments. Should different growth factors be used, there is no evidence showing that the FeHNTs would prevent differentiation into other types of tissues. In fact, due to the FeHNTs ability to adsorb different molecules on the surface, this could allow for a controlled development of bone tissues should the FeHNTs with adsorbed growth factors be used in a calcium phosphate cement (CPC) scaffold [9, 10].

5.3 Future Research

FeHNTs present great potential for combating osteosarcoma. There should be further investigation into using FeHNTs in tissue scaffolds, as the tissue scaffolds do allow for the ability to quickly regenerate lost tissue, as well as their effect on vital organs. This material, due to its unique properties in combating cancerous growth and tissue healing, could potential be used to combat other cancers. Osteosarcoma is usually

adherent, as are other sarcomas, lymphomas, melanomas, and carcinomas. Cancer cells had already been shown to be negatively affected by oscillation of a magnetic field in in Ashdown et al., 2020, where the authors we able to rupture the cells membrane of three different types of carcinoma cells while lymphatic endothelial cells were unaffected [12].

As well, the ability to cause hyperthermia should be further examined. For instance, if medical personnel are able to surround malignant growth with the FeHNTs, there could be a way to detach the growth by causing the outer cells to undergo necrosis. This would cause little to no damage to healthy tissue, while also removing most cancerous cells in one procedure. The uptake of FeHNTs by cancerous and healthy cells must be examined before this method can be examined.

Finally, the addition of anti-cancer drugs to FeHNT for use in neoadjuvant chemotherapy treatments should be examined, as the combination of hyperthermia and anti-cancer drugs can allow for much more efficiency in combatting cancer cell growth and limiting its spread outside the localized region [3]. With the rupturing of cancer cell membranes, this could provide a treatment that may not need surgical resection and make surgical reconstruction and tissue regeneration a much easier task.

BIBLIOGRAPHY

[1] M. S. Isakoff, S. S. Bielack, P. Meltzer, and R. Gorlick, "Osteosarcoma: Current treatment and a collaborative pathway to success," *Journal of Clinical Oncology*, vol. 33, no. 27, pp. 3029–3035, 2015.

[2] R. A. Durfee, M. Mohammed, and H. H. Luu, "Review of osteosarcoma and current management," *Rheumatology and Therapy*, vol. 3, no. 2, pp. 221–243, Oct. 2016.

[3] R. D. Issels, L. H. Lindner, J. Verweij, P. Wust, P. Reichardt, B.-C. Schem, S. Abdel-Rahman, S. Daugaard, C. Salat, C.-M. Wendtner, Z. Vujaskovic, R. Wessalowski, K.-W. Jauch, H. R. Dürr, F. Ploner, A. Baur-Melnyk, U. Mansmann, W. Hiddemann, J.-Y. Blay, and P. Hohenberger, "Neo-adjuvant chemotherapy alone or with regional hyperthermia for localised high-risk soft-tissue sarcoma: A randomised phase 3 multicentre study," *The Lancet Oncology*, vol. 11, no. 6, pp. 561–570, Jun. 2010.

[4] V. Spina, N. Montanari, and R. Romagnoli, "Malignant tumors of the osteogenic matrix," *European Journal of Radiology*, vol. 27, pp. S98–S109, May 1998.

[5] Q. A. Pankhurst, J. Connolly, S. K. Jones, and J. Dobson, "Applications of Magnetic Nanoparticles in Biomedicine," *Journal of Physics D: Applied Physics*, vol. 36, pp. R167–R181, Jun. 2003.

[6] A. Seifalian, E. Bull, S. Y. Madani, R. Sheth, M. Green, and A. Seifalian, "Stem cell tracking using iron oxide nanoparticles," *International Journal of Nanomedicine*, vol. 2014, no. 9, pp. 1641–1653, Mar. 2014.

[7] X. Li, Z. Wei, H. Lv, L. Wu, Y. Cui, H. Yao, J. Li, H. Zhang, B. Yang, and J. Jiang, "Iron oxide nanoparticles promote the migration of mesenchymal stem cells to injury sites," *International Journal of Nanomedicine*, vol. 14, pp. 573–589, Jan. 2019.

[8] Y. Xia, H. Chen, Y. Zhao, F. Zhang, X. Li, L. Wang, M. D. Weir, J. Ma, M. A. Reynolds, N. Gu, and H. H. K. Xu, "Novel magnetic calcium phosphate-stem cell construct with magnetic field enhances osteogenic differentiation and bone tissue engineering," *Materials Science and Engineering: C*, vol. 98, pp. 30–41, Dec. 2018.

[9] Y. Xia, J. Sun, L. Zhao, F. Zhang, X.-J. Liang, Y. Guo, M. D. Weir, M. A. Reynolds, N. Gu, and H. H. K. Xu, "Magnetic field and nano-scaffolds with stem cells to enhance bone regeneration," *Biomaterials*, vol. 183, pp. 151–170, Aug. 2018.

[10] Y. Xia, Y. Guo, Z. Yang, H. Chen, K. Ren, M. D. Weir, L. C. Chow, M. A. Reynolds, F. Zhang, N. Gu, and H. H. K. Xu, "Iron oxide nanoparticle-calcium phosphate cement enhanced the osteogenic activities of stem cells through Wnt/β-catenin signaling," *Materials Science and Engineering: C*, vol. 104, pp. 1–14, Jul. 2019.

[11] Y. Shen, R. Xia, H. Jiang, Y. Chen, L. Hong, Y. Yu, Z. Xu, and Q. Zeng, "Exposure to 50hz-sinusoidal electromagnetic field induces DNA damage-independent autophagy," *The International Journal of Biochemistry & Cell Biology*, vol. 77, pp. 72–79, May 2016.

[12] C. P. Ashdown, S. C. Johns, E. Aminov, M. Unanian, W. Connacher, J. Friend, and M. M. Fuster, "Pulsed low-frequency magnetic fields induce tumor membrane disruption and altered cell viability," *Biophysical Journal*, vol. 118, no. 7, pp. 1552–1563, Feb. 2020.

[13] M. Fizir, P. Dramou, K. Zhang, C. Sun, C. Pham-Huy, and H. He, "Polymer grafted-magnetic halloysite nanotube for controlled and sustained release of Cationic Drug," *Journal of Colloid and Interface Science*, vol. 505, pp. 476–488, Nov. 2017.

[14] P. Dramou, M. Fizir, A. Taleb, A. Itatahine, N. S. Dahiru, Y. A. Mehdi, L. Wei, J. Zhang, and H. He, "Folic acid-conjugated chitosan oligosaccharide-magnetic halloysite nanotubes as a delivery system for Camptothecin," *Carbohydrate Polymers*, vol. 197, pp. 117–127, May 2018.

[15] N. S. Hwang, C. Zhang, Y. S. Hwang, and S. Varghese, "Mesenchymal stem cell differentiation and roles in Regenerative Medicine," *Wiley Interdisciplinary Reviews: Systems Biology and Medicine*, vol. 1, no. 1, pp. 97–106, 2009.

[16] L. da Silva Meirelles, A. I. Caplan, and N. B. Nardi, "In search of the in vivo identity of mesenchymal stem cells," *Stem Cells*, vol. 26, pp. 2287–2299, Jun. 2008.

[17] V. V. Miana and E. A. Prieto González, "Adipose tissue stem cells in regenerative medicine," *ecancermedicalscience*, vol. 12, no. 822, pp. 1–14, Mar. 2018.

[18] M. Saler, L. Caliogna, L. Botta, F. Benazzo, F. Riva, and G. Gastaldi, "hASC and DFAT, Multipotent Stem Cells for Regenerative Medicine: A Comparison of Their Potential Differentiation In Vitro," *International Journal of Molecular Sciences*, vol. 18, pp. 2699–2714, Dec. 2017.

[19] T. Onda, O. Honmou, K. Harada, K. Houkin, H. Hamada, and J. D. Kocsis, "Therapeutic benefits by human mesenchymal stem cells (hMSCs) and ang-1 gene-modified hMSCs after cerebral ischemia," *Journal of Cerebral Blood Flow & Metabolism*, vol. 28, no. 2, pp. 329–340, Feb. 2007.

[20] D. K. Mills, Y. Luo, A. Elumalai, S. Esteve, S. Karnik, and S. Yao, "Creating structured hydrogel microenvironments for regulating stem cell differentiation," *Gels*, vol. 6, no. 47, pp. 1–18, Dec. 2020.

[21] P. A. Dresco, V. S. Zaitsev, R. J. Gambino, and B. Chu, "Preparation and properties of magnetite and polymer magnetite nanoparticles," *Langmuir*, vol. 15, no. 6, pp. 1945–1951, Feb. 1999.

[22] L. Néel, "Antiferromagnetism and ferrimagnetism," *Proceedings of the Physical Society*. Section A, vol. 65, no. 11, pp. 869–885, Nov. 1952.

[23] S. Satish, M. Tharmavaram, and D. Rawtani, "Halloysite nanotubes as a nature's boon for biomedical applications," *Nanobiomedicine*, vol. 6, pp. 1–16, Jun. 2019.

[24] K. Fakhruddin, R. Hassan, M. U. Khan, S. N. Allisha, S. I. Razak, M. H. Zreaqat, H. F. Latip, M. N. Jamaludin, and A. Hassan, "Halloysite nanotubes and Halloysite-based composites for biomedical applications," *Arabian Journal of Chemistry*, vol. 14, no. 9, pp. 1–20, Jul. 2021.

[25] A. Karewicz, A. Machowska, M. Kasprzyk, and G. Ledwójcik, "Application of halloysite nanotubes in cancer therapy—A Review," *Materials*, vol. 14, no. 11, pp. 1–24, 2021.

[26] M. Massaro, R. Noto, and S. Riela, "Past, present and future perspectives on Halloysite Clay Minerals," *Molecules*, vol. 25, no. 20, p. 4863, 2020.

[27] G. Gastaldi, A. Asti, M. F. Scaffino, L. Visai, E. Saino, A. M. Cometa, and F. Benazzo, "Human adipose-derived stem cells (hASCs) proliferate and differentiate in osteoblast-like cells on trabecular titanium scaffolds," *Journal of Biomedical Materials Research Part A*, vol. 94A, no. 3, pp. 790–799, Sep. 2010.

[28] E. G. Tzortzaki, A. V. Koutsopoulos, K. I. Dambaki, I. Lambiri, M. Plataki, M. K. Gordon, D. R. Gerecke, and N. M. Siafakas, "Active remodeling in idiopathic interstitial pneumonias: Evaluation of collagen types XII and XIV," *Journal of Histochemistry and Cytochemistry*, vol. 54, no. 6, pp. 693–700, Jul. 2006.

[29] J. P. Gleeson, N. A. Plunkett, and F. J. O'Brien, "Addition of hydroxyapatite improves stiffness, interconnectivity and osteogenic potential of a highly porous collagen-based scaffold for bone tissue regeneration," *European Cells and Materials*, vol. 20, pp. 218–230, Jul. 2010.